EPJ Web of Conferences **182**, 02129 (2018) https://doi.org/10.1051/epjconf/201818202129
ICNFP 2017

Understanding $X(3862)$, $X(3872)$, and $X(3930)$ spectrum in a Friedrichs-model-like scheme

Zhiguang Xiao[1,a] and Zhi-Yong Zhou[2,b]

[1] *Interdisciplinary Center for Theoretical Study, University of Science and Technology of China, Hefei, Anhui 230026, China*
[2] *School of Physics, Southeast University, Nanjing 211189, P. R. China*

Abstract. In this talk, we review the method we proposed to use the Friedrichs-like model combined with QPC model to include the hadron interaction corrections to the spectrum predicted by the quark model, in particular the Godfrey-Isgur model. This method is then used on the first excited P-wave charmonium states, and $X(3862)$, $X(3872)$, and $X(3930)$ state could be simultaneously produced with a quite good accuracy. The $X(3872)$ state is shown to be a bound state with a large $D\bar{D}^*$ continuum component. At the same time, the $h_c(2P)$ state is perdicted at about 3902 MeV with a pole width of about 54 MeV.

1 Introduction

Recent years have seen more and more exotic hadron states which can not be satisfactorily described by the naïve quark model. In general, for states below the open-flavor threshold, the mass spectra predicted using the quark model, such as the Godfrey-Isgur(GI) model [3], agree well with the experimental results. However, above or near the open-flavor threshold, general discrepancies between the quark-model predictions and the experimental results appear and there are also new states which can not be incorporated in the quark model. Some typical examples are the first excited P-wave charmonium states, i.e. $n^{2s+1}L_J = 2^3P_2, 2^3P_1, 2^3P_0$, and 2^1P_1 charmonium states. The mass of the well-accepted $\chi_{c2}(2P)$ state, also known as $X(3930)$, discovered by the Belle Collaboration in $\gamma\gamma \to D\bar{D}$[1], is about 50 MeV lower than the prediction in the quark potential model [2–4]. The properties of the other P-wave states have not been firmly determined yet. The famous $X(3872)$, first observed in the $B^\pm \to K^\pm J/\psi\pi^+\pi^-$ by the Belle Collaboration in 2003 [5], just locates around the $D\bar{D}^*$ threshold. Although its quantum number is confirmed to be 1^{++}[6, 7], the same as the $\chi_{c1}(2P)$, the pure charmonium interpretation has been deemed as "improbable" for its unexpected mass, width and the isospin violation. In fact, Törnqvist proposed the existence of a $D\bar{D}^*$ molecular state with $J^{PC} = 1^{++}$ near $D\bar{D}^*$ threshold about ten years before $X(3872)$ was discovered [8]. However, the pure molecular state explanation also encounters difficulties in understanding its prompt production[9] and radiative decays[10, 11]. So the nature of the $X(3872)$ is still obscure up to now. Another puzzling state $X(3915)$ used to be assigned to $\chi_{c0}(2P)$, but this assignment was also doubted. The mass splitting between the $\chi_{c2}(2P)$ and the $X(3915)$ is too small compared to the $1P$ correspondence. It was

[a] e-mail: xiaozg@ustc.edu.cn
[b] e-mail: zhouzhy@seu.edu.cn

discovered in the $X(3915) \to J/\psi\omega$ decay modes which is OZI suppressed but lack of the evidence in the OZI allowed $X(3915) \to D\bar{D}$ mode [12, 13]. These are unexpected from theoretical point of view. The $J^{PC} = 0^{++}$ assignment to $X(3915)$ is based on the analysis of the angular distribution data from *BABAR* Collaboration [14] with a very low statistics. In Ref.[15], the angular distribution of $X(3915)$ to the final leptonic and pionic states was reanalyzed without the helicity-2 dominance assumption and the results also support the possibility of assigning it to a 2^{++} state, which means that it might be the same tensor state as the $X(3930)$. Very recently, the Belle Collaboration announced a new candidate for the $\chi_{c0}(2P)$, $X(3862)$, with a mass 3862^{+66}_{-45}MeV and width 201^{+242}_{-149} MeV [16]. There is another $2P$ state $h_c(2P)$ with $J^{PC} = 1^{+-}$ which is expected by the quark model but has not been discovered in the experiments yet. For more detailed discussions on these puzzles, the readers are referred to some recent reviews for example refs. [17–19].

One of the reasons why the quark model such as the GI model [3] can not describe the states above the open-flavor well is the neglect of the interactions between the hadrons. These interactions will in general introduce the momentum dependent corrections to the hadron propagators and hence will modify the spectrum. For hadrons below the open-flavor threshold, the modifications play the role of renormalization of mass and may roughly be absorbed into the constants in the original quark potential model. However, for hadrons above the open-flavor threshold, the energy dependence of the self-energy function can not be neglected. In this work, we will adopt a solvable extended Friedrichs model [20–22] combined with the Quark Pair Creation (QPC) model to incorporate this effect into the hadron spectra above the open-flavor threshold and use it to study the $2P$ charmonium-like states as an application. Our method uses the eigenvalues and wave functions for mesons in the GI model [3] as input to the Friedrichs model and QPC model, the latter of which is used to describe the interaction between the hadrons. Thus, this method can be viewed as a kind of correction to GI's relativized quark model. Applying this method on the $2P$ charmonium-like states, we found that the first excited 2^{++}, 1^{++}, and 0^{++} charmonium states could be reproduced with good accuracy in a one parameter calculation, and the mass and the width of 1^{+-} state are also obtained as a prediction.

These results are helpful in resolving the long-standing puzzle of identifying the observed first excited P-wave state, and also shed more light on the interpretation of the enigmatic $X(3872)$ state. Furthermore, this method provides a general way to incorporate the hadron interaction corrections to the spectra predicted by the quark model, and can be used in evaluating the other mass spectra above the open-flavor threshold and reconciling the gaps between the quark potential model predictions and the experimental results.

2 Friedrichs-like model

In this section, we review some basic facts of the Friedrichs model [23] and some of its generalizations developed in [20–22]. The simplest version of the Friedrichs model considers the interaction between a discrete state $|0\rangle$ and a continuum state $|\omega\rangle$. The the full Hamiltonian H is separated into a free part and an interaction part as

$$H = H_0 + V. \tag{1}$$

H_0 is the free Hamiltonian

$$H_0 = \omega_0|0\rangle\langle 0| + \int_{\omega_{th}}^{\infty} \omega|\omega\rangle\langle\omega| d\omega \tag{2}$$

where the eigenvalues for the free Hamiltonian are ω_0 for the discrete state, and ω for the continuum eigenstate satisfying $\omega \in [\omega_{th}, \infty)$, ω_{th} being the threshsold for the continuum states. These states are

normalized as

$$\langle 0|0\rangle = 1, \langle \omega|\omega'\rangle = \delta(\omega - \omega'), \langle 0|\omega\rangle = \langle \omega|0\rangle = 0. \tag{3}$$

The interaction part can be expressed as

$$V = \lambda \int_{\omega_{th}}^{\infty} [f(\omega)|\omega\rangle\langle 0| + f^*(\omega)|0\rangle\langle\omega|]\mathrm{d}\omega, \tag{4}$$

where $f(\omega)$ function denotes the coupling form factor between the discrete state and the continuum state, and λ denotes the coupling strength. The eigenvalue problem for the full Hamiltonian can be exactly solved and the solutions include a continuum spectrum and a discrete spectrum. The final eigenstates of the continuum spectrum with eigenvalue $E > \omega_{th}$ can be expressed as

$$|\Psi_{\pm}(E)\rangle = |E\rangle + \lambda \frac{f(E)}{\eta^{\pm}(E)}\Big[|\omega_0\rangle + \lambda \int_0^{\infty} \mathrm{d}\omega \frac{f(\omega)}{E - \omega \pm i\epsilon}|\omega\rangle\Big], \tag{5}$$

where

$$\eta^{\pm}(x) = x - \omega_0 - \lambda^2 \int_0^{\infty} \frac{f(\omega)f^*(\omega)}{x - \omega \pm i\epsilon}\mathrm{d}\omega \tag{6}$$

and are normalized as $\langle \Psi_{\pm}(E)|\Psi_{\pm}(E')\rangle = \delta(E - E')$. The subscript $\pm$ denotes the in-states $(+)$ and outstates $(-)$, respectively. The S-matrix can also be obtained as

$$S(E, E') = \delta(E - E')\left(1 - 2\pi i \frac{\lambda f(E) f^*(E)}{\eta^+(E)}\right). \tag{7}$$

The $\eta^{\pm}$ function can be analytically continued to the complex plane to be one complex function $\eta(z)$ for $z \in \mathbb{C}$ with its boundary $\eta(x \pm i\epsilon) = \eta^{\pm}(x)$ for $x \in \mathbb{R}$. Since there is only one threshold for the continuum, there is only one cut for this function, and $\eta(z)$ will be defined on a two-sheeted Riemann surface. The zero points for the $\eta(z) = 0$ will be the poles for the S-matrix. As expected, by directly solving the eigenvalue problem, the zero points of $\eta(z)$ or the pole positions for the S-matrix will be the eigenvalues for the full Hamiltonian and represent the generalized discrete spectrum for the Hamiltonian. Depending on the position of the solution, different kinds of the discrete generalized eigenstates can be found:

1. Bound state.

   The solution to $\eta(z) = 0$ on the first sheet real axis and below ω_{th} represents a bound state. The wave function solution is expressed as

   $$|z_B\rangle = N_B\Big(|0\rangle + \lambda \int_{\omega_{th}}^{\infty} \frac{f(\omega)}{z_B - \omega}|\omega\rangle\mathrm{d}\omega\Big), \tag{8}$$

   This solution has a finite norm and can be normalized as $\langle z_B|z_B\rangle = 1$ when $N_B = (\eta'(z_B))^{-1/2} = \left(1 + \lambda^2 \int d\omega \frac{|f(\omega)|^2}{(z_B - \omega)^2}\right)^{-1/2}$ is chosen. Thus this is a well-defined state vector in the Hilbert space. Then, it is easy to define the so-called "elementariness" Z and "compositeness" X,

   $$Z = N_B^2, \quad X = \lambda^2 N_B^2 \int d\omega \frac{|f(\omega)|^2}{(z_B - \omega)^2}. \tag{9}$$

   The physical meaning for the elementariness is the probability of finding the original discrete state in the bound state and the compositeness is the probability for finding the original continuum states in the bound state.

2. Virtual state.

   If the solution lies on the real axis below the threshold on the second sheet, it represents a virtual state. The wave function can also be expressed as

$$|z_V^{\pm}\rangle = N_V\Big(|0\rangle + \lambda \int_{\omega_{th}}^{\infty} \frac{f(\omega)}{z_V^{\pm} - \omega}|\omega\rangle \mathrm{d}\omega\Big), \tag{10}$$

   where the superscript ± denotes the two kinds of integration contours which are continued from the upper side (+) or the lower side (−) of cut on the first sheet to the second sheet, enclosing the virtual state pole position. Unlike the bound state, virtual state does not have a well-defined norm as the usual states in the Hilbert space. Thus, the compositeness and elementariness for the virtual state can not be mathematically rigorously defined. However, we can define a normalization such that $\langle z_V^-|z_V^+\rangle = 1$, by choosing $N_V = (\eta'^+(z_V))^{-1/2} = \left(1 + \lambda^2 \int d\omega \frac{|f(\omega)|^2}{[z_V^+ - \omega]^2}\right)^{-1/2}$.

3. Resonant state.

   If there is a solution on the second sheet complex plane there must be another mirror image with respect to the real axis because of the real analyticity of η function. This pair of poles represent a resonance since it is unstable due to the finite imaginary part of the energy eigenvalue. The pole position is related to the mass M and width Γ as $z = M - i\frac{\Gamma}{2}$. The wave functions for the two poles can be expressed as

$$\begin{aligned} |z_R\rangle &= N_R\Big(|0\rangle + \lambda \int_{\omega_{th}}^{\infty} \mathrm{d}\omega \frac{f(\omega)}{[z_R - \omega]_+}|\omega\rangle\Big), \\ |z_R^*\rangle &= N_R^*\Big(|0\rangle + \lambda \int_{\omega_{th}}^{\infty} \mathrm{d}\omega \frac{f^*(\omega)}{[z_R^* - \omega]_-}|\omega\rangle\Big), \end{aligned} \tag{11}$$

   where z_R is on the lower half plane and z_R^* is its complex conjugate. The $[\cdots]_{\pm}$ means the analytical continuations of the integration from upper or lower edge of the first sheet cut [20]. Similar to the virtual states, the wave functions for the resonance can not be normalized as usual, and thus are not the normal state vector in the Hilbert space. However we can also choose $N_R = (\eta'^+(z_R))^{-1/2} = \left(1 + \lambda^2 \int d\omega \frac{|f(\omega)|^2}{[(z_R - \omega)_+]^2}\right)^{-1/2}$ to normalize the state as $\langle z_R^*|z_R\rangle = 1$. Notice that the normalization N_R will be complex in general. If one also defines the elemetariness and compositeness as in Eq. (9), they will become complex and thus may not have well-defined physical meaning. However, some definitions proposed in the literature [24, 25] might be able to approximately describe these physical quantities.

These discrete spectrum solutions may or may not be generated from the orignal discrete state. If the state is generated from the bare discrete state, it will move back to the bare state if one decreases the coupling to zero. The discrete states can also be dynamically generated from the singularities of the form factor. If we tune the coupling to zero, the positions of this kind of states may move towards the singularity of the form factor on the unphysical sheets, no matter the singularity is located at finite position or at infinity[20, 21]. From above solutions, we see that only the bound states can have well-defined norms as usual state vectors in the Hilbert space, while virtual states and resonances are not the usual states in the Hilbert space. To describe these two kinds of states, the rigged-Hilbert-space (RHS) formulation of the quantum mechanics was developed by Bohm and Gadella [26, 27]. The discrete resonant state and virtual states are generalized eigenstate for the full Hamiltonian. In particular, the resonant state is also called Gamow state and the virtual state is also called antibound

state. These states are described using the space of the anti-linear continuous functionals ($\Omega^{\times}$) of a kernel space (Ω) of the original Hilbert space ($\mathcal{H}$), and the three spaces construct the Gel'fand triplet $\Omega \subset \mathcal{H} \subset \Omega^{\times}$ [26]. By summing up the perturbation series, I. Prigogine and his collaborators also obtained similar solutions [28].

In above discussions, the continuum states are labeled only by the energy quantum number which seems to be unrelated to the states in the three dimensional space. In fact, after partial-wave decomposition of the three dimensional states, the similar model for the three dimensional states is reduced to a Friedrichs-like model [22]. Consider the continuum momentum eigenstate $|\vec{p}, S, S_z\rangle$, with a total spin S and z-component S_z, where $\pm\vec{p}$ are the center of mass (c.m.) momenta for the two particles which compose the continuum state. The discrete state denoted by $|0, JM\rangle$ also has a spin quantum number J and the magnetic quantum number M. In the nonrelativistic theory, the free Hamiltonian in the c.m. system can be expressed as

$$H_0 = M_0 \sum_M |0; JM\rangle\langle 0; JM| + \sum_{S_z} \int \mathrm{d}^3 p\, \omega |\vec{p}; S\, S_z\rangle\langle \vec{p}; S\, S_z|\,, \tag{12}$$

where M_0 is the bare mass of the discrete state and $\omega = M_{th} + \frac{p^2}{2\mu}$ is the energy of the continuum state in the c.m. frame, M_{th} being the threshold energy of the two-particle states and μ being the reduced mass in the c.m. frame. The continuum state can be decomposed into the angular momentum eigenstates,

$$|\vec{p}; S\, S_z\rangle = \sum_{JM, LM_L} i^L Y_L^{M_L *}(\hat{p}) C^{JM}_{LM_L, S\, S_z} |p; JM; LS\rangle\,, \tag{13}$$

where $C^{JM}_{LM_L, S\, S_z}$ is the Clebsch-Gordan coefficient. After this partial-wave decomposition, this free Hamiltonian can be expressed in the angular momentum representation as

$$H_0 = M_0 \sum_M |0; JM\rangle\langle 0; JM| + \sum_{j,m;L} \int p^2 \mathrm{d}p\, \omega |p; jm; LS\rangle\langle p; jm; LS|\,, \tag{14}$$

With the rotational symmetry of the interaction between the discrete state and the continuum, the matrix elements of the potential can be expressed as

$$\langle 0; JM|V|\vec{p}; S\, S_z\rangle = \sum_{LM_L} i^L \tilde{f}_L(p^2) C^{JM}_{LM_L, S\, S_z} Y_L^{M_L *}(\hat{p})\,. \tag{15}$$

The interaction term of the Hamiltonian can then be expressed as

$$\begin{aligned} H_{01} &= \sum_{S_z, M} \int \mathrm{d}^3 p |0; JM\rangle\langle 0; JM|V|\vec{p}; S\, S_z\rangle\langle \vec{p}; S\, S_z| + h.c. \\ &= \sum_{L,M} \int \mu p \mathrm{d}\omega \tilde{f}_L(p^2) |0; JM\rangle\langle p; JM; LS| + h.c. \end{aligned} \tag{16}$$

Since we consider only fixed total angular momentum quantum numbers JM and fixed S, by redefining $|0\rangle = |0; JM\rangle$, $|\omega, L\rangle = \sqrt{\mu p}|p; JM; LS\rangle$ and $f(\omega) = \sqrt{\mu p}\tilde{f}(\omega)$, the total Hamiltonian for fixed JM can be recast into

$$H = M_0 |0\rangle\langle 0| + \sum_L \int \mathrm{d}\omega\, \omega |\omega, L\rangle\langle \omega, L| + \sum_L \int d\omega f_L(\omega) |0\rangle\langle \omega, L| + h.c. \tag{17}$$

This is just similar to the original Friedrichs model but with more continua, and the similar exact solution can be obtained.

We can make more generalizations by adding more discrete states and more continuum states, and the interactions between continuum states can also be introduced. The most general Hamiltonian with D discrete states, $|i\rangle$ ($i = 1, \ldots, D$), and C continuum states, $|\omega_j, j\rangle$ ($j = 1, \ldots, C$), can be expressed as

$$H = \sum_{i=1}^{D} M_i|0;i\rangle\langle 0;i| + \sum_{i=1}^{C}\int_{M_{i,th}}^{\infty} d\omega_i\omega_i|\omega_i;i\rangle\langle\omega_i;i| \tag{18}$$

$$+ \sum_{i_2,i_1}\int_{M_{i_1,th}} \mathrm{d}\omega' \int_{M_{i_2,th}} \mathrm{d}\omega\, g_{i_2,i_1}(\omega',\omega)|\omega';i_2\rangle\langle\omega;i_1| + h.c. \tag{19}$$

$$+ \sum_{i=1}^{D}\sum_{j=1}^{C}\int_{M_{j,th}} d\omega f_{i,j}(\omega)|0;i\rangle\langle\omega;j| + h.c. \tag{20}$$

where $f_{i,j}(\omega)$ is the form factor describing the interaction between the ith descrete state and the jth continuum state, and g_{ij} discribes the interaction between the ith continuum and the jth continuum. For general interations g_{ij}, the model is not solvable, but if $g_{ij}(\omega',\omega) = v_{ij}f_i(\omega')f_j(\omega)$ and $f_{ij} = u_{ij}f_j(\omega)$, where u_{ij} and v_{ij} are constant, the model can also be exactly solved. See Ref. [22] for details. In the following, we will consider the case where there is only one discrete state coupled with several continuum states and no interactions between the continuum states. The solutions differ from the ones previously described by simply adding more similar continuum integrals in Eqs. (5), (6), (8), (10), (11). Since there could be more than one threshold for the continuum state, each new threshold will double the number of the Riemann sheets and the poles on the original Riemann sheets will also be copied to the new sheets and be renormalized differently. So, one bare state could correspond to more than one poles on different sheets and will be renormalized differently becoming so-called shadow poles [29]. But only the ones near the physical region could have observable effects. For more detailed discussion, the readers are referred to Ref. [22].

We will restrict our study on the properties of mesons. The next problem is to determine the interaction between the discrete meson state and the continuum states which are composed of two mesons. We will use the QPC model [30] to model this kind of interaction. In this model, the meson coupling $A \to BC$ can be defined as the transition matrix element

$$\langle BC|T|A\rangle = \delta^3(\vec{P_f} - \vec{P_i})\mathcal{M}^{ABC} \tag{21}$$

where the transition operator T in the QPC model is defined as

$$T = -3\gamma\sum_m \langle 1m1-m|00\rangle \int d^3\vec{p_3}d^3\vec{p_4}\delta^3(\vec{p_3}+\vec{p_4})\mathcal{Y}_1^m(\frac{\vec{p_3}-\vec{p_4}}{2})\chi_{1-m}^{34}\phi_0^{34}\omega_0^{34}b_3^\dagger(\vec{p_3})d_4^\dagger(\vec{p_4}), \tag{22}$$

describing a quark-antiquark pair generated by the $b_3^\dagger$ and $d_4^\dagger$ creation operators from the vacuum. χ_{1-m}^{34} and ω_0^{34} are the spin wave function and the color wave function, respectively. $\mathcal{Y}_1^m$ is the solid Harmonic function. γ parameterizes the production strength of the quark-antiquark pair. The definition of the meson state here is a little different from the one in Ref. [31] by omitting the factor $\sqrt{2E}$ to ensure the correct normalizations,

$$|A(n,{}^{2S+1}L_{J,M})(\vec{P})\rangle = \sum_{M_L,M_S}\langle LM_LSM_S|JM\rangle \int d^3p\,\psi_{nLM_L}(\vec{p})\chi_{SM_S}^{12}\,\phi^{12}\,\omega^{12}$$
$$\times\Big|q_1\Big(\frac{m_1}{m_1+m_2}\vec{P}+\vec{p}\Big)\bar{q}_2\Big(\frac{m_2}{m_1+m_2}\vec{P}-\vec{p}\Big)\Big\rangle.$$

χ^{12} is the spin wavefunction. ϕ^{12} is the isospin wave function. ω^{12} is the color wave function. p_1 (p_2) and m_1 (m_2) are the momentum and mass of the quark (anti-quark). $\vec{P} = \vec{p}_1 + \vec{p}_2$ is the momentum of the center of mass, and $\vec{p} = \frac{m_2\vec{p}_1 - m_1\vec{p}_2}{m_1+m_2}$ is the relative momentum. ψ_{nLM_L} is the spatial wave function for the meson, n being the radial quantum number.

By the standard derivation one can obtain the amplitude $\mathcal{M}^{ABC}$ defined by Eq. (21) and the partial-wave amplitude $\mathcal{M}^{SL}(P(\omega))$ as in Ref. [30]. Then the form factor f_{SL} which describes the interaction between $|A\rangle$ and $|BC\rangle$ in the Friedrichs model can be obtained as

$$f_{SL}(\omega) = \sqrt{\mu P(\omega)}\mathcal{M}^{SL}(P(\omega)), \tag{23}$$

where $P(\omega) = \sqrt{\frac{2M_BM_C(\omega - M_B - M_C)}{M_B+M_C}}$ is the c.m. momentum, M_B and M_C being the masses of meson B and C respectively.

The wave funtions describing the meson states in the QPC model will be given by the GI model [3]. The GI model partially relativizes the linear confinement, Coulomb-type, and color-hyperfine interactions, and provides very successful predictions to the mass spectra of the conventional meson states composed of u, d, s, c, and b quarks, but its predictions with regard to the states above the open-flavor thresholds are not as good as those below. These discrepancies might arise from the neglect of the coupling between these "bare" meson states and their decay channels as they mentioned [3]. In our scheme, the GI's Hamiltonian which provides the discrete bare hadron eigenstates can be effectively viewed as the free Hamiltonian in the Friedrichs model, and the interactions between the bare states of H_0 and the continuum states is modeled by the QPC model and thus will provide the corrections to the mass spectra. Since the OZI-allowed channel will be more strongly coupled to the bare states than the OZI-suppressed channel, the pole shift is dominantly caused by these OZI-allowed channels. So, we include only the OZI-allowed channels in our analysis.

3 First excited P-wave charmonium states

After all the theoretical preparation, we will use our method in the analysis of the spectrum of P-wave charmonium states. There are four different channels with different quantum numbers, 2^1P_1, $2^3P_{0,1,2}$. The coupled channels are chosen up to $D^*\bar{D}^*$ in these four cases. The $\chi_{c2}(2P)$ state can couple to $D\bar{D}$, $D\bar{D}^*$, and $D^*\bar{D}^*$ in both S and D-wave. For the $\chi_{c1}(2P)$ and $h_c(2P)$ states, the coupled channels are $D\bar{D}^*$, and $D^*\bar{D}^*$. In the case of the $\chi_{c0}(2P)$ state, the coupled channels are $D\bar{D}$, and $D^*\bar{D}^*$. To describe these interactions using the QPC model, we need the wave functions for the bare charmonium states and the charmed mesons. Using the parameters given in the GI model [3], we first reproduced GI's results by approximating the wave function of the P-wave charmonium states and the charmed mesons with 30 Harmonic Oscillator wave function basis. Using these wave functions as input in the QPC model, one could then obtain the coupling form factor in the Friedrichs model. The only parameter of the QPC model is γ, which represents the quark pair production strength from the vacuum. In the literature, various values of γ are chosen in different situations, and a typical value is chosen as 6.9 [4, 32]. However, since the wave functions used here are different from theirs, there is no need to choose the same value as there. We choose it to be a value around 4 such that all the observed P-wave first excited charmonium state spectrum can be reproduced well simultaneously in our scheme [33].

As stated in the previous section, the generalized eigenvalues of the full Hamiltonian can be solved by finding the zero points of the $\eta(z)$ function on the complex energy plane, which are also the poles of the scattering amplitude. These eigenevalues give the pole masses and pole widths for the states. Since in experiments, the mass distribution is ususally fitted by Breit-Wigner parametrization, we also

calculate the Breit-Wigner mass which is determined by solving [34, 35]

$$M_{BW} - \omega_0 - \sum_n \mathcal{P} \int_{\omega_{th,n}}^{\infty} \frac{\sum_{SL} |f^n_{SL}(\omega)|^2}{M_{BW} - \omega} \mathrm{d}\omega = 0, \tag{24}$$

on the real axis where $\mathcal{P}\int$ means principal value integration, and the Breit-Wigner partial width of the n-th open channel is expressed as

$$\Gamma^n_{BW} = 2\pi \sum_{S,L} |f^n_{SL}(M_{BW})|^2, \tag{25}$$

with the total width given by $\Gamma_{tot} = \sum_n \Gamma^n_{BW}$. The numerical results of the extracted pole positions and the corresponding Breit-Wigner parameters are shown in Table 1.

Table 1. Comparison of the experimental masses and the total widths (in MeV) [36] with our results.

$n^{2s+1}L_J$	M_{expt}	Γ_{expt}	M_{BW}	Γ_{BW}	pole	GI
2^3P_2	3927.2 ± 2.6	24 ± 6	3920	10	3920-4i	3979
2^3P_1	3942 ± 9	37^{+27}_{-17}			3934-40i	3953
	3871.69 ± 0.17	< 1.2	3871	0	3871-0i	
2^3P_0	3862^{+66}_{-45}	201^{+242}_{-149}	3878	11	3878-5i	3917
2^1P_1			3895	37	3902-27i	3956

For the 2^3P_2 channel, $D\bar{D}$ and $D\bar{D}^*$ thresholds are open for the $\chi_{c2}(2P)$. The mass is shifted from the GI's value 3979 MeV down to around 3920 MeV, about 7 MeV below the observed value. Its width is about 10 MeV, a little smaller than the experimental one. The branching ratio between $D\bar{D}$ and $D\bar{D}^*$ estimated using Eq. (25) is 2.4 which demonstrates that $D\bar{D}$ is its dominant decay product. This is as expected since the coupling to $D\bar{D}^*$ is through D-wave interaction, while the coupling to $D\bar{D}$ is through S wave. Though its decay rate to $D\bar{D}^*$ is relatively small, $X(3930)$ may still have a small contribution to the $D\bar{D}^*$ mass distribution, which might be detected in the experiments.

In the 2^3P_1 channel, the bare state is shifted down from GI's value 3953 MeV to about 3934 MeV with a fairly large width. Meanwhile, another bound state pole emerges just below the threshold around 3871 MeV, which is consistent with the $X(3872)$ found in the experiment. So, it is natural to assign this bound state pole to the $X(3872)$. If the coupling strength γ is tuned a little smaller, this bound-state pole will move across the $D\bar{D}^*$ threshold to the second sheet and becomes a virtual state pole. So, we may not exclude the possibility of a virtual state nature [37]. This state is dynamically generated from the form factor, thus from the interaction between the discrete state and the continuum in the s channel, which is an evidence of the molecular origin of the $X(3872)$. This picture is a little different from the pion exchange picture [8] which is a t-channel process. The higher state generated from GI's bare $\chi_{c1}(2P)$ state is rather broad indicating its strong coupling with $D\bar{D}^*$. It might be related to the $X(3940)$ state.

One of the advantage of using the Friedrichs model is that we can find the wave function for the bound state and the compositeness and elementariness are well-defined in this case as shown in Eq.(9). Since $X(3872)$ in our results is a bound state, we can estimate the compositeness and elementariness for it. It is easy to find that the relative ratio of finding $c\bar{c}$ and $D\bar{D}^*$ in the state is about $1 : 3.1 \sim 1 : 9.3$ if we tune the γ parameter such that the $X(3872)$ locates within $3871.0 \sim 3871.7$MeV, indicating the dominance of the continuum part in this state, which also demonstrates its molecule dominant

nature [8, 38–40]. That this ratio is sensitive to the position of the $X(3872)$ is because that it is very close to the threshold and thus will affect the integral a lot.

In the 2^3P_0 channel, our result shows that the $\chi_{c0}(2P)$ state is shifted from GI's prediction 3917 MeV to about 3878 MeV but has a very narrow width, about 11 MeV. Recently, by analysing the $e^+e^- \to J/\psi D\bar{D}$ data, Belle collaboration accounced a new $\chi_{c0}(2P)$ candidate with a mass 3862^{+66}_{-45} MeV and a width of a large uncertainty, 201^{+242}_{-149} MeV [16], which consists with our result. In our calculation, we find that the coupling of the $\chi_{c0}(2P)$ to the $D\bar{D}$ is unexpectedly small from the QPC model using GI's wavefunctions, which causes its width to be rather small. This narrow width is roughly only the bin size of the present announced data and the statistics of the data in this region may not be enough. So, more data with higher resolution are needed to determine whether there is a narrow signal in this region. An interesting observation is that there seems to be a small excess at the vicinity of about 3860 MeV in the $\gamma\gamma \to D\bar{D}$ experiment of both Belle [1] and *BABAR* Collaboration [41] as shown in Fig. 1. Especially in *BABAR*'s data, the small structure extends to a dip around 3880MeV.

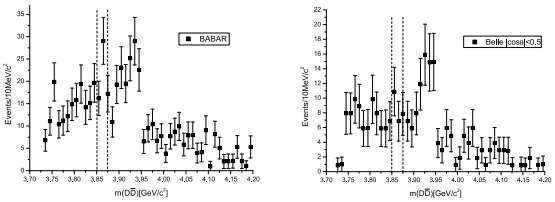

Figure 1. The mass distribution of $\gamma\gamma \to D\bar{D}$ from *BABAR* [41] and Belle [1]. The data of Belle is the one for $|\cos\theta^*| < 0.5$. The two dashed lines are set at $m(D\bar{D}) = 3850$ MeV and 3875 MeV.

The $h_c(2P)$ state is predicted at around 3902 MeV with a narrow width about 54 MeV. As we have mentioned, $\chi_{c2}(2P)$, $\chi_{c1}(2P)$, $h_c(2P)$ are very close to each other and all couple to the $D\bar{D}^*$ channel, which has no definite C-parity. This means that the enhancement above the DD^* threshold contains all the contributions from these states. To detect the $h_c(2P)$ signal, one needs to look for it in a channel with a definite negative C-parity such as $\eta_c\gamma$ or $J/\psi\pi^0$ in this energy region. However, the neutral $X(3900)$ can also decay to $J/\psi\pi^0$. So, it is difficult to distinguish these two states in $J/\psi\pi^0$. In fact, it is really impossible to achieve this from the low statistics data for $\psi(4160) \to \pi^0\pi^0 J/\psi$ from BES [42]. If $X(3900)$ is believed to be of molecular nature, it may not be easy to decay to $\eta_c\gamma$. Thus, $\eta_c\gamma$ may be a good channel to look for $h_c(2P)$.

4 Conclusion

In this talk, we first reviewed a general method to introduce the hadronic interaction corrections to the spectra predicted by the quark model, in particular, the well-accepted GI's relativized quark model, using the Friedrichs-like model combined with the QPC model. Then we use this scheme on the excited P-wave charmonium-like states, and found that the experimental observed states could be simultaneously reproduced. In this scheme, the $X(3872)$ state is a dynamically generated bound state by the coupling between the bare $\chi_{c1}(2P)$ state and continuum states. The compositeness and elementariness can also be obtained and it is found that the continuum component are dominant, which indicates its molecular nature. But the $\chi_{c1}(2P)$ becomes a resonance at about 3934 MeV with a width of about 80. The $\chi_{c0}(2P)$ is found to be an unexpectedly narrow one and the mass is consistent with

the recently announced $\chi_{c0}(2P)$ candidate by Belle. We also predict that the mass of the unobserved $h_c(2P)$ is at about 3902 MeV and its pole width is about 54 MeV.

Since we have obtained the wave function of the $X(3872)$ in terms of bare discrete states and bare continuum states, more properties of $X(3872)$ can be studied based on this information. In a subsequent work [43], we studied the isospin breaking effect of the $X(3872)$ based on the same scheme, and find that the result is consistent with the experimental data.

5 Acknowledgments

Z.X. is supported by China National Natural Science Foundation under contract No. 11105138, 11575177 and 11235010. Z.Z is supported by the Natural Science Foundation of Jiangsu Province under contract No. BK20171349.

References

[1] S. Uehara et al. (Belle Collaboration), Phys.Rev.Lett. **96**, 082003 (2006), hep-ex/0512035
[2] E. Eichten, K. Gottfried, T. Kinoshita, K.D. Lane, T.M. Yan, Phys. Rev. **D 17**, 3090 (1978), [Erratum: Phys. Rev.D 21,313(1980)]
[3] S. Godfrey, N. Isgur, Phys. Rev. **D 32**, 189 (1985)
[4] T. Barnes, S. Godfrey, E.S. Swanson, Phys. Rev. **D 72**, 054026 (2005), hep-ph/0505002
[5] S.K. Choi et al. (Belle Collaboration), Phys. Rev. Lett. **91**, 262001 (2003), hep-ex/0309032
[6] R. Aaij et al. (LHCb), Phys. Rev. Lett. **110**, 222001 (2013), 1302.6269
[7] R. Aaij et al. (LHCb), Phys. Rev. **D 92**, 011102 (2015), 1504.06339
[8] N.A. Tornqvist, Z. Phys. **C61**, 525 (1994), hep-ph/9310247
[9] C. Bignamini, B. Grinstein, F. Piccinini, A.D. Polosa, C. Sabelli, Phys. Rev. Lett. **103**, 162001 (2009), 0906.0882
[10] E.S. Swanson, Phys. Lett. **B598**, 197 (2004), hep-ph/0406080
[11] Y. Dong, A. Faessler, T. Gutsche, V.E. Lyubovitskij, J. Phys. **G38**, 015001 (2011), 0909.0380
[12] F.K. Guo, U.G. Meissner, Phys.Rev. **D 86**, 091501 (2012), 1208.1134
[13] S.L. Olsen, Phys. Rev. **D 91**, 057501 (2015), 1410.6534
[14] J. Lees et al. (*BABAR* Collaboration), Phys.Rev. **D 86**, 072002 (2012), 1207.2651
[15] Z.Y. Zhou, Z. Xiao, H.Q. Zhou, Phys. Rev. Lett. **115**, 022001 (2015), 1501.00879
[16] K. Chilikin et al. (Belle), Phys. Rev. **D 95**, 112003 (2017), 1704.01872
[17] S.L. Olsen, T. Skwarnicki, D. Zieminska (2017), 1708.04012
[18] H.X. Chen, W. Chen, X. Liu, S.L. Zhu, Phys. Rept. **639**, 1 (2016), 1601.02092
[19] R.F. Lebed, R.E. Mitchell, E.S. Swanson, Prog. Part. Nucl. Phys. **93**, 143 (2017), 1610.04528
[20] Z. Xiao, Z.Y. Zhou, Phys. Rev. **D 94**, 076006 (2016), 1608.00468
[21] Z. Xiao, Z.Y. Zhou, J. Math. Phys. **58**, 062110 (2017), 1608.06833
[22] Z. Xiao, Z.Y. Zhou, J. Math. Phys. **58**, 072102 (2017), 1610.07460
[23] K.O. Friedrichs, Commun. Pure Appl. Math. **1**, 361 (1948)
[24] T. Sekihara, T. Hyodo, D. Jido, PTEP **2015**, 063D04 (2015), 1411.2308
[25] Z.H. Guo, J.A. Oller, Phys. Rev. **D 93**, 096001 (2016), 1508.06400
[26] A. Bohm, M. Gadella, *Dirac Kets, Gamow Vectors and Gel'fand Triplets*, Vol. 348 of *Lecture Notes in Physics* (Springer Berlin Heidelberg, 1989), ISBN 978-3-540-51916-4 (Print) 978-3-540-46859-2 (Online)

[27] O. Civitarese, M. Gadella, Phys. Rep. **396**, 41 (2004)
[28] T. Petrosky, I. Prigogine, S. Tasaki, Physica **173A**, 175 (1991)
[29] R.J. Eden, J.R. Taylor, Phys. Rev. **133**, B1575 (1964)
[30] H.G. Blundell, S. Godfrey, Phys. Rev. **D 53**, 3700 (1996), hep-ph/9508264
[31] C. Hayne, N. Isgur, Phys. Rev. **D 25**, 1944 (1982)
[32] R. Kokoski, N. Isgur, Phys. Rev. **D 35**, 907 (1987)
[33] Z.Y. Zhou, Z. Xiao, Phys. Rev. **D96**, 054031 (2017), 1704.04438
[34] M.R. Pennington, D.J. Wilson, Phys. Rev. **D 76**, 077502 (2007), 0704.3384
[35] N.A. Tornqvist, Z. Phys. **C68**, 647 (1995), hep-ph/9504372
[36] C. Patrignani et al., Chin. Phys. **C40**, 100001 (2016)
[37] C. Hanhart, Yu.S. Kalashnikova, A.E. Kudryavtsev, A.V. Nefediev, Phys. Rev. **D 76**, 034007 (2007), 0704.0605
[38] D. Gamermann, J. Nieves, E. Oset, E.R. Arriola, Phys. Rev. **D 81**, 014029 (2010), 0911.4407
[39] F.K. Guo, C. Hanhart, U.G. MeiSSner, Q. Wang, Q. Zhao, Phys. Lett. **B725**, 127 (2013), 1306.3096
[40] C. Meng, H. Han, K.T. Chao (2013), 1304.6710
[41] B. Aubert et al. (*BABAR* Collaboration), Phys.Rev. **D 81**, 092003 (2010), 1002.0281
[42] T. Xiao, S. Dobbs, A. Tomaradze, K.K. Seth, Phys. Lett. **B727**, 366 (2013), 1304.3036
[43] Z.Y. Zhou, Z. Xiao (2017), 1711.01930